land

MDPI

Article

Multi-Scenario Simulation of Land-Use/Land-Cover Changes and Carbon Storage Prediction Coupled with the SD-PLUS-InVEST Model: A Case Study of the Tuojiang River Basin, China

Qi Wang [1,†], Wenying Zhang [1,†], Jianguo Xia [1], Dinghua Ou [1,2], Zhaonan Tian [1] and Xuesong Gao [1,2,*]

[1] College of Resources, Sichuan Agricultural University, Chengdu 611130, China; qiwang@sicau.edu.cn (Q.W.); 2020206033@stu.sicau.edu.cn (W.Z.); 10083@sicau.edu.cn (J.X.); 14340@sicau.edu.cn (D.O.); 71410@sicau.edu.cn (Z.T.)
[2] Key Laboratory of Investigation, Monitoring, Protection and Utilization for Cultivated Land Resources, Ministry of Natural Resources, Chengdu 610045, China
* Correspondence: xuesonggao@sicau.edu.cn
† These authors contributed equally to this work.

Abstract: Land-use and land-cover changes (LUCCs) significantly impact carbon sequestration by modifying the structure and function of terrestrial ecosystems. This study utilized GIS and remote sensing techniques to forecast future LUCC patterns and their influence on regional carbon budgets, which is essential for sustainable development. We devised a coupled system dynamics (SD) model integrated with a patch-generating land-use simulation (PLUS) model to simulate LUCCs under diverse future scenarios using multisource environmental data. Additionally, the InVEST model was employed to quantify carbon storage in terrestrial ecosystems. By establishing three scenarios—ecological priority (EP), highly urbanized (HU), and coordinated development (CD)—this study's aim was to predict the LUCC patterns and carbon storage distribution of the Tuojiang River Basin (TRB), China, up to 2035. The results showed that (1) from 2000 to 2020, significant LUCCs occurred in the TRB, primarily involving the conversion of cultivated land into construction areas and forestland; (2) LUCCs had a substantial impact on carbon storage in the TRB, with the EP scenario demonstrating the highest carbon storage by 2035 due to extensive forest expansion, while the HU scenario indicated a decline in carbon storage associated with rapid urbanization; and (3) the mountainous regions of the TRB, dominated by forestland, consistently exhibited higher carbon storage, whereas the Chengdu Plain region in the upper basin displayed the lowest. In conclusion, we recommend prioritizing the CD scenario in future development strategies to balance economic growth with ecological protection while simultaneously enhancing carbon storage. Our findings offer valuable insights to shape future LUCC policies in the Tuojiang River Basin, underscoring the adaptability of the coupled model approach to a wide range of geographic scales and contexts.

Keywords: land use; coupling model; ecological protection; scenario prediction; remote sensing; carbon sequestration

check for updates

Citation: Wang, Q.; Zhang, W.; Xia, J.; Ou, D.; Tian, Z.; Gao, X. Multi-Scenario Simulation of Land-Use/Land-Cover Changes and Carbon Storage Prediction Coupled with the SD-PLUS-InVEST Model: A Case Study of the Tuojiang River Basin, China. *Land* **2024**, *13*, 1518. https://doi.org/10.3390/land13091518

Academic Editors: Xinhai Lu and Danling Chen

Received: 30 July 2024
Revised: 27 August 2024
Accepted: 9 September 2024
Published: 19 September 2024

Copyright: © 2024 by the authors. Licensee MDPI, Basel, Switzerland. This article is an open access article distributed under the terms and conditions of the Creative Commons Attribution (CC BY) license (https://creativecommons.org/licenses/by/4.0/).

1. Introduction

Global climate change has emerged as an increasingly pressing concern, impeding human activities and posing significant challenges to sustainable development [1]. China has underscored its commitment to achieving peak carbon emissions around 2030 and attaining carbon neutrality by approximately 2060 [2]. Terrestrial ecosystems play a key role in addressing the challenges presented by global warming and in achieving regional carbon balances by serving as a crucial carbon sink [3,4]. Through an analysis of the correlation between carbon storage and LUCCs, we gained valuable insights into response dynamics and spatial distribution patterns, facilitating more effective monitoring of regional carbon

changes [5]. The incorporation of anticipated land-use changes into ecosystem carbon storage assessments has proven to be a vital strategy, offering a primary approach to optimizing land patterns to enhance carbon sequestration.

The significant alteration in LUCC changes has a profound impact on regional carbon sequestration by restructuring ecosystem composition and function, thus influencing terrestrial carbon storage and release processes [6,7]. The conversion of natural lands, such as forests and grasslands, into cultivated land generally leads to reduced soil carbon stocks [8,9]. Conversely, in semi-arid and arid regions, the transformation of these lands into cropland can result in increased SOC levels [10]. Previous studies have frequently neglected changes in land-use transformation patterns driven by various future development strategies, mainly focusing on the assessment and modeling of historical land use [11]. The intricate characteristics of human–environment systems, coupled with the uncertainty of future land-use changes, present challenges in understanding the spatiotemporal patterns of carbon budgets resulting from these changes [12]. Recently, land-use models have emerged as crucial technical approaches to investigate the processes and mechanisms underlying LUCCs and discerning their ecological implications [13]. In forecasting land use, vital considerations are needed to predict structural compositions and simulate spatial distribution patterns [14,15]. Traditional methods, such as the Markov model, which is used to forecast land demand, have limitations in effectively accounting for socioeconomic development factors [16]. In contrast, the system dynamics (SD) model proficiently accommodates system complexities, delineating time-series relationships and capturing nonlinear effects [17]. It also excels at scenario design and provides decision-making support [18]. Furthermore, the advanced patch-generating land-use simulation (PLUS) method excels in simulating spatial distribution patterns, accurately capturing the impact of various LUCCs and allowing for precise modeling of patch-level changes [19]. Consequently, the integration of the SD and PLUS models from the perspective of systemic integrity—encompassing social, economic, and ecological sustainability—provides a robust approach to accurately predict land-use demands and capture spatial distribution changes across various future scenarios [20,21].

Different methodologies have been employed to investigate carbon storage in terrestrial ecosystems, such as field sampling [22], remote sensing estimations [23], and empirical statistical models [24]. However, challenges arise in their applicability to long-term regional soil carbon estimation studies due to issues related to data accessibility and usability [25]. With advancements in remote sensing technology and increased accessibility to Earth observation data, the integrated valuation of ecosystem services and trade-offs (InVEST) model is notable for its effectiveness at calculating carbon storage [26]. Its significant advantages include the requirement of fewer data inputs and a rapid operational speed, making it a suitable candidate for application across large spatial scales for the assessment of carbon storage [27,28]. Combining land-use change models with the InVEST model has the potential to enhance the management of terrestrial ecosystem carbon sequestration under current policies or potential future scenarios, thereby providing guidance to achieve high-quality regional development [29].

Situated in the upper reaches of the Yangtze River, the Tuojiang River Basin (TRB) holds significant importance for green and low-carbon developments and serves as a vital ecological barrier of the upper Yangtze River. In recent decades, population growth and economic development have accelerated rapid industrialization and urbanization, posing a threat to terrestrial ecosystem carbon sinks [3]. Based on this background, this study employed a coupled SD-PLUS–InVEST model alongside remotely sensed multisource environmental data to achieve three main objectives: (1) identifying the spatiotemporal characteristics of LUCCs in the TRB from 2000 to 2020, (2) simulating LUCC spatial patterns under various scenarios in 2035, and (3) predicting and analyzing carbon storage dynamics from 2000 to 2035 under different scenarios. Our findings provide valuable scientific guidance for policy incentives and sustainable development advancements in the basin.

2. Materials and Methods

2.1. Study Area

The TRB (28°52′ N–31°42′ N, 103°40′ E–105°45′ E) is located in the upper stream of the Yangtze River, covering an area of around 2.79 × 10^4 km^2, and contains 27 complete counties (Figure 1). The region experiences a range of climatic conditions, primarily a humid subtropical monsoon climate with an annual average temperature ranging from 15.7 to 18.2 °C and an annual average precipitation ranging from 870 mm to 1700 mm. The basin topography descends from northwest to southeast and features diverse topography, including highlands in the northwest and lowlands in the southeast, encompassing mountains, plains, and hills. The TRB serves as an important ecological screen and economic center in the upper Yangtze River Region [30]. Although it constitutes only 5.74% of the total area of Sichuan Province, the basin contributes considerably to the economic output and population of the province, accounting for approximately 30% and 28%, respectively. Since the 21st century, human activities have substantially impacted economic development and population expansion, leading to profound shifts in land-use patterns and carbon storage [31,32]. Achieving a balance between economic progress and ecological conservation, along with heightened efforts toward carbon neutrality, is crucial for the region.

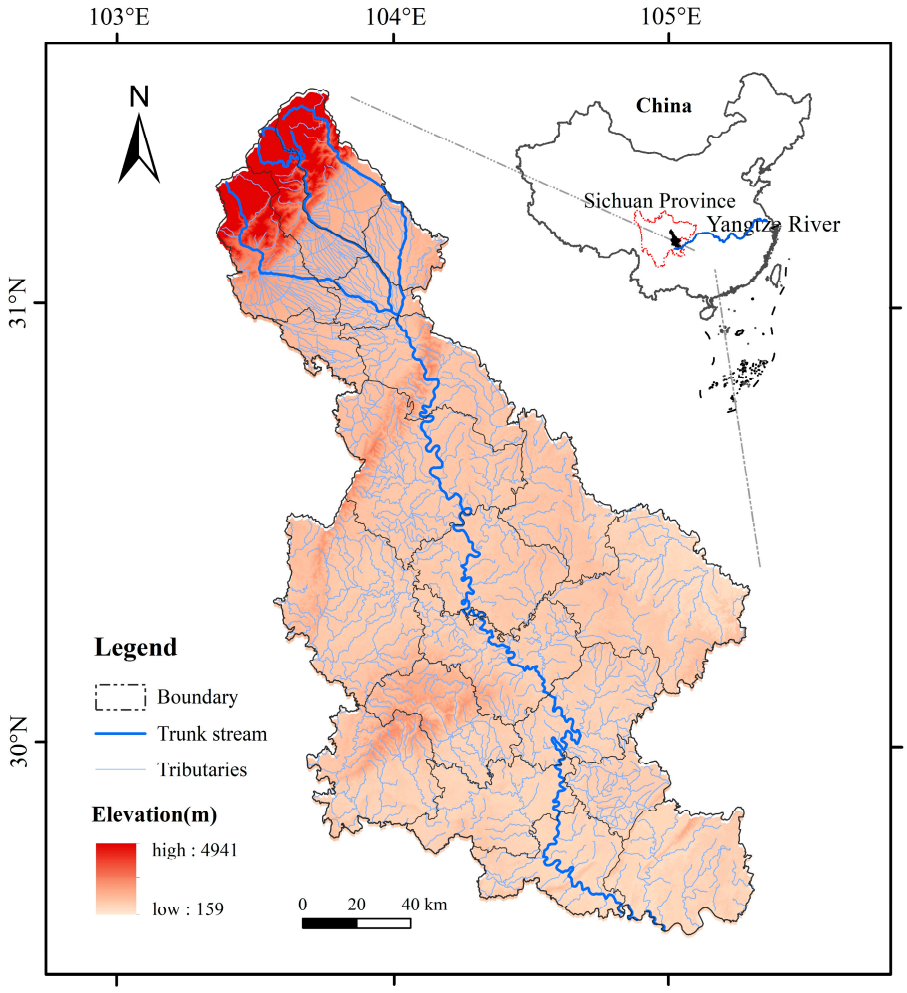


Figure 1. Overview of the study area.

2.2. Data Sources

This study employs a system dynamics approach to partition the study area into three subsystems: population, economy, and land use. Consistent with prior research [33], thirteen variables were selected to represent three primary aspects: population growth,

economic development, and land-use patterns. Population growth is primarily denoted by population density, which also partially reflects labor force concentration. Economic development is gauged using GDP and the intensity of nighttime human activities. Land-use patterns, primarily serving industrial and agricultural purposes, are influenced by transportation and labor for industrial development and by topography and climate for agricultural development. The selected factors encompass slope, elevation, soil type, NDVI, annual precipitation, annual temperature, GDP, population density, nighttime light index, and distance to highways, national roads, provincial roads, and county roads.

Table 1 provides details of the sources and essential information concerning the LUCCs and driving factors utilized in the PLUS model. The LUCC data from 2000 to 2020 were acquired from the China Land Cover Dataset (CLCD), derived from Landsat images available on the Google Earth Engine. Previous studies typically used time-sectional data, making it difficult to capture land-use changes over consecutive years. The CLCD dataset offers continuous time-series data, enabling a more precise comprehension of historical land-use change patterns, as compared to conventional time-sectional data [34]. The CLCD dataset achieved a comprehensive accuracy rate of 79.31% based on the interpretation of over 5000 samples. Socioeconomic and meteorological data required for the SD model from 2000 to 2020 were obtained from the "Sichuan Statistical Yearbook".

Table 1. Details of spatial data used for the study.

Data Type	Data	Year	Resolution	Sources
Land use	Land use	2000–2020	30 m	CLCD dataset from Yang and Huang [34]
Natural factors	DEM	2020	30 m	Geospatial Data Cloud (https://www.gscloud.cn, accessed on 15 March 2023)
	Temperature	2000–2020	1 km	National Earth System Science Data Center (http://www.geodata.cn, accessed on 10 March 2023)
	Precipitation	2000–2020	1 km	
	Soil type	1995	1 km	Resource and Environment Science and Data Center (https://www.resdc.cn/, accessed on 20 March 2023)
	GDP	2019	1 km	
	Population density	2000–2020	100 m	
Socio-economic factors	NDVI	2020	250 m	National Aeronautics and Space Administration (https://modis.gsfc.nasa.gov/data/, accessed on 15 March 2023)
	Nighttime light	2015	30 m	National Earth System Science Data Center (http://www.geodata.cn, accessed on 5 March 2023)
	Traffic network	2020	30 m	OpenStreetMap (https://www.openhistoricalmap.org, accessed on 5 March 2023)

To ensure data consistency, all spatial data were resampled to a 30-meter spatial resolution using the nearest-neighbor method. They were then re-projected to a standardized coordinate system (WGS 1984, UTM Zone 48).

2.3. Research Protocol

The proposed integrated protocol in this study comprises the following three steps (Figure 2): (1) Based on the characteristics of land-use changes in the TRB from 2000 to 2020, we identified the interactions among different components of the human–land system and employed the SD model to simulate land-use demand under specified scenarios. (2) After validation, the PLUS model was employed to simulate the spatial patterns of LUCCs in 2035. (3) The InVEST model was used to estimate both historical and future changes in carbon storage across different scenarios.

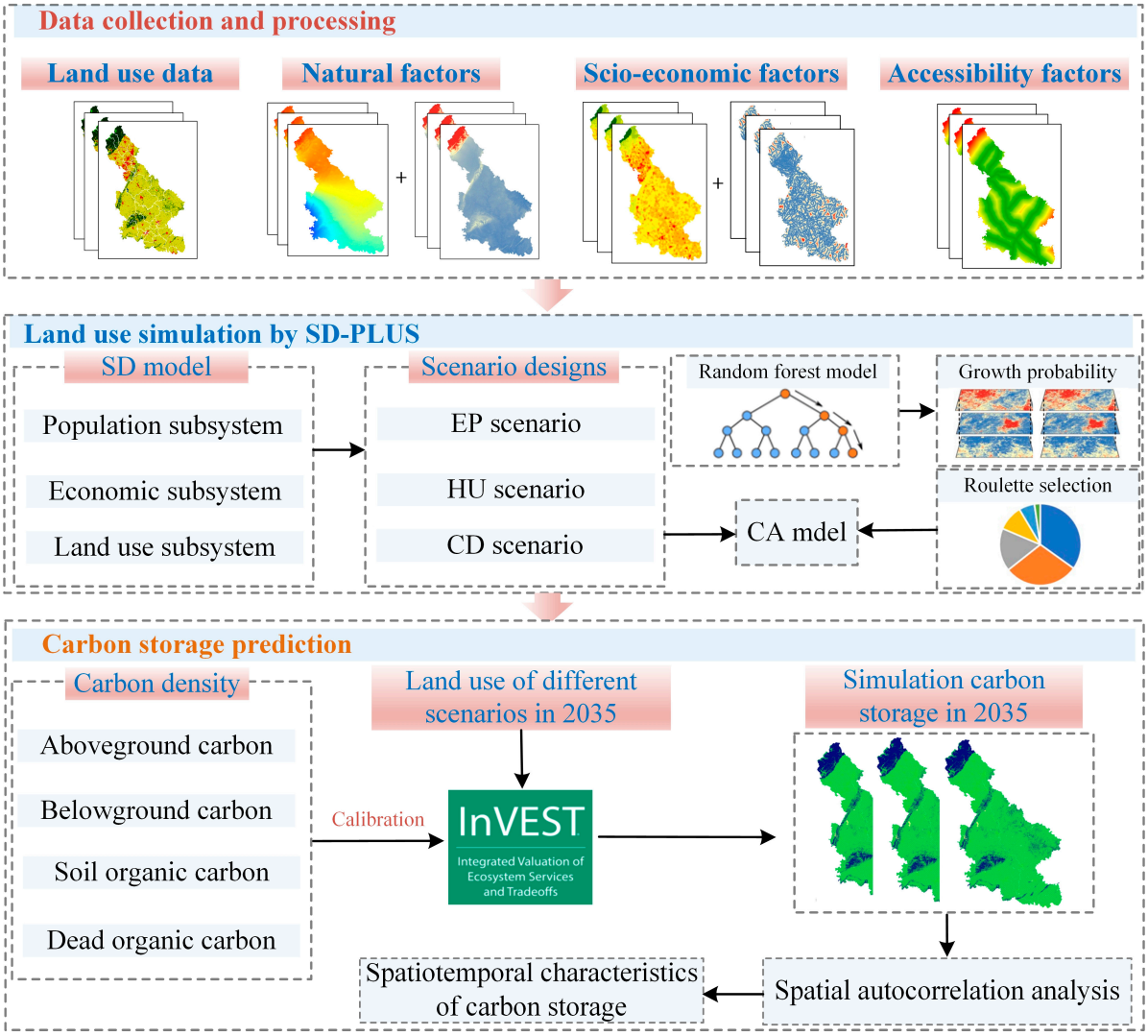


Figure 2. Research framework.

2.3.1. Optimization of LUCC Structure Using SD Model

The established SD model included three subsystems, population, economy, and land, and is utilized to analyze the most substantial interactions and feedback among various elements based on land-use change, population growth, and economic development features in the TRB from 2000 to 2020 through a causal loop diagram. These interactions are depicted through a system dynamics causal loop diagram (Supplementary Materials Figure S1). Based on the causal loop diagram, 8 state variables, 11 rate variables, 27 auxiliary variables, and 2 constants (Supplementary Materials Table S1) were chosen to construct the SD model using Vensim PLE software (version 5.1) for the TRB (Supplementary Materials Figure S2). Comparisons were made between the simulated and observed LUCC data for 2020 to assess the accuracy of the simulation. Different scenarios with adjusted parameters were used to simulate projected changes in land-use quantity demand.

2.3.2. Simulation of Spatial Land-Use Changes Using the PLUS Model

The PLUS model incorporates a rule mining framework using the Land Expansion Analysis Strategy (LEAS) model alongside a Cellular Automaton (CA) model that utilizes multitype Random Seeds (CARS) [19]. Through the application of random forest classification, LEAS assesses the effects of driving factors on land-use changes and calculates the likelihood of land development. The CARS model calculates the overall probability for various land-use types based on neighborhood effects, land-use development probabili-

ties, and adaptive coefficients. Previous investigations have demonstrated that the PLUS model exhibits superior performance in simulating diverse land-use changes at the patch level, resulting in heightened simulation accuracy and a more authentic representation of landscape patterns [19].

The scenario setting considers policy factors. Considering that China's national economic planning operates at five-year intervals, the scenario settings in this study were structured around five-year periods. Combining the 14th Five-Year Plan and the overarching Long-Range Goal for 2035 in China and Sichuan Province, different scenarios were set as follows:

Ecological priority scenario (EP): This scenario implements rigorous protective measures for cultivated and ecological land while constraining the swift expansion of construction land. We chose a low GDP growth and urbanization rate coupled with a high agricultural land structure factor to safeguard cultivated land. Additionally, we emphasize the protection of ecological land by selecting a high per-capita forestland ratio.

High urbanization scenario (HU): This scenario emphasizes rapid economic development without compromising agricultural growth and ecological protection. Therefore, we opted for a high GDP growth rate and urbanization rate to signify rapid economic progress. A low agricultural land structure factor was selected to maintain a minimum baseline for arable land. To stabilize the per-capita ecological land baseline while ensuring gradual improvement, we chose low-per-capita forest land, moderate-per-capita grassland, and moderate-per-capita water areas.

Coordinated development scenario (CD): In pursuit of sustainable development that harmonizes ecological preservation and economic advancement, we chose a moderate GDP growth rate and moderate urbanization rate to denote high-quality economic development. Selecting a moderate agricultural land structure factor ensures that the arable land meets the demands of both economic development and high-quality agricultural growth. Additionally, opting for moderate-per-capita forest land, high-per-capita grassland, and high-per-capita water areas signifies an augmentation of per-capita ecological land levels.

Various parameters were set based on historical land transfer probabilities and related studies in the TRB, incorporating high-, moderate-, and low-level values (Tables S2–S4).

Using 2010 as the baseline and 2020 as the validation year, the accuracy of the PLUS model was tested. The model's performance in simulating land-use patterns was assessed using the Kappa and Figure of Merit (FoM) coefficients [35,36]. The Kappa coefficient, which varies between 0 and 1, signifies a higher simulation accuracy with a larger value. When the FoM value was close to or greater than 20%, the model demonstrated credibility and applicability [37,38].

2.3.3. Simulation of Carbon Storage with InVEST Model

A carbon calculation module within the InVEST model is used to estimate carbon storage. Carbon storage estimates in the InVEST model encompassed the following fundamental carbon pools: soil organic matter, aboveground, belowground, and dead organic matter. Carbon storage was calculated using the following equation:

$$C_i = C_{soil} + C_{above} + C_{below} + C_{dead} \quad (1)$$

$$C_{total} = \sum_{i=1}^{n} C_i \times A_i, (i = 1, 2, \ldots, n) \quad (2)$$

where C_i is the total carbon density for LUCC type i (Mg·hm^{-2}); C_{soil} represents soil organic carbon density for LUCC type i (Mg·hm^{-2}); C_{above} represents the aboveground carbon density for LUCC type i (Mg·hm^{-2}); C_{below} represents the underground carbon density for LUCC type i (Mg·hm^{-2}); C_{dead} represents the dead organic carbon density for LUCC type i (Mg·hm^{-2}); C_{total} represents the total terrestrial ecosystem carbon stocks (Mg); A_i represents the area of LUCC type i (hm^2).

The carbon density of each land-use type within our study region was obtained from previous studies in Sichuan Province, to which our research area belongs [39–43]. Due to the modulation of local climatic conditions on soil organic carbon storage [44], we simultaneously applied a climate correction model [45,46] to calibrate the carbon density in the TRB. The correction coefficient formulas are as follows:

$$K_{BP} = \frac{0.03 \times P_1 + 14.4}{0.03 \times P_2 + 14.4}, K_{BT} = \frac{-0.4 \times T_1 + 43.0}{-0.4 \times T_2 + 43.0}, K_B = \text{Average}(K_{BP}, K_{BT}) \quad (3)$$

$$K_{SP} = \frac{0.07 \times P_1 + 79.1}{0.07 \times P_2 + 79.1}, K_{ST} = \frac{-3.4 \times T_1 + 157.7}{-3.4 \times T_2 + 157.7}, K_S = \text{Average}(K_{SP}, K_{ST}) \quad (4)$$

$$K_{DP} = \frac{0.001 \times P_1 + 0.58}{0.001 \times P_2 + 0.58}, K_{DT} = \frac{-0.03 \times T_1 + 2.03}{-0.03 \times T_2 + 2.03}, K_D = \text{Average}(K_{DP}, K_{DT}) \quad (5)$$

where P_1 and P_2 are annual average precipitation (mm) in the TRB and Sichuan Province; T_1 and T_2 are annual average temperature in the TRB and Sichuan Province (°C); K_{BP} and K_{BT} are the biomass correction coefficients corresponding to the precipitation and temperature, respectively; K_B is the average correction coefficient for biomass carbon density; K_{SP} and K_{ST} are the soil correction coefficients corresponding to the precipitation and temperature, respectively; K_S is the average correction coefficient for soil carbon density; K_{DP} and K_{DT} are the dead correction coefficients corresponding to the precipitation and temperature, respectively; K_D is the average correction coefficient for dead organic matter.

Finally, the calibrated carbon density data in the TRB were estimated by multiplying the correction coefficient by the above carbon density data (Table 2).

Table 2. The calibrated carbon density for various land-use types in the TRB (Mg C·hm^{-2}).

Land Use Type	C_{above}	C_{below}	C_{soil}	C_{dead}
Cultivated land	38.24	79.73	91.13	0.99
Forest	54.89	143.13	202.53	3.46
Grassland	28.95	52.27	132.44	0.99
Water	0.28	0.97	16.64	1.17
Construction land	3.26	86.25	113.11	0
Unused land	22.33	135.26	168.54	0

2.3.4. Spatial Autocorrelation Analysis

Carbon density was aggregated at the town level using ArcGIS software (version 10.2), and global autocorrelation was conducted through Moran's I value using GeoDa software (version 1.14). Moran's I value, which falls within the range of [−1, 1], is utilized to investigate the existence of a spatial agglomeration model in the carbon storage pattern within the TRB. Finally, the local autocorrelation results were obtained using Local Moran's I, and spatial patterns of carbon storage were identified through the use of LISA aggregation graphs.

3. Results

3.1. Land-Use Change during 2000–2035

3.1.1. Land-Use Change during 2000–2020

The Sankey diagram (Figure 3) elucidates the characteristics of the land-use structure within the TRB over two decades. Cultivated land is predominant in the TRB, constituting more than 80% of the total area. Forestland is the second most common land type, accounting for approximately 11% of the land. Other land categories collectively account for less than 6% of the total area. From 2000 to 2020, cultivated land in the TRB decreased by 1340.84 km^2, while the construction land and forest increased by 744.49 km^2 and 555.40 km^2, respectively.

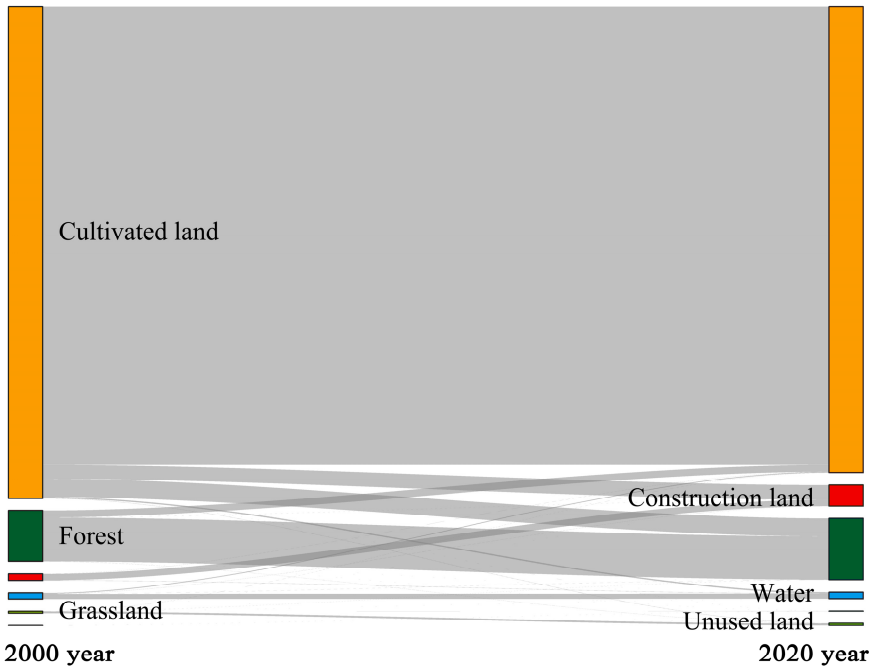


Figure 3. Sankey diagram of land-use change during 2000 to 2020 in the Tuojiang River Basin.

3.1.2. Simulation of Land-Use Change under Different Scenarios

Using the PLUS model, we simulated the 2020 land-use map based on the 2010 land-use data. Subsequently, the simulation outcomes were then compared with the actual 2020 land-use map data to assess and evaluate the model's performance. The analysis revealed that the PLUS model attained an overall simulation accuracy of 0.92, accompanied by a Kappa coefficient of 0.83. The obtained FoM value was 0.19, which is similar to those reported in other simulation studies [47,48]. Therefore, it shows the reliability of the FLUS model in forecasting the spatial dynamics of LUCCs.

By 2035, the land-use composition within the TRB will be dominated by cultivated land and forests (Table 3). Compared with 2020, the construction land area increases by 508.93 km², 734.00 km², and 966.92 km² under the EP, CD, and HU scenarios, respectively, corresponding to growth rates of 45.99%, 66.33%, and 87.37%. Under the HU scenario, the growth in construction land was most significant, with the noticeable expansion concentrated in the Chengdu Plain metropolitan area in the upper reaches of the TRB (Figure 4). Under the three scenarios, the area of cultivated land is expected to decrease to different extents, with expected reductions of 617.34 km^2, 802.14 km^2, and 996.04 km^2, respectively. Under the EP scenario, forestland will increase the most by 119.78 km^2 compared to 2020, with an increase rate of 3.71%. Over the next 30 years, there will be a continual reduction in grassland areas. Furthermore, no distinct trend was observed in water or unused land from 2020 to 2035. Overall, future land-use changes in the TRB will mainly focus on the transition between cultivated land, forests, and construction land, with cultivated land being the primary changing land category.

Table 3. Land area of different types under the three scenarios projected for 2035 (km^2).

Land Use Type	2020	EP	HU	CD
Cultivated land	24,665.24	24,047.90	23,669.20	23,863.10
Forest	3231.27	3351.05	3264.07	3307.92
Grassland	112.73	102.00	102.11	101.92
Water	338.49	341.10	348.55	343.95
Construction land	1106.65	1615.58	2073.57	1840.65
Unused land	5.29	1.59	1.71	1.68

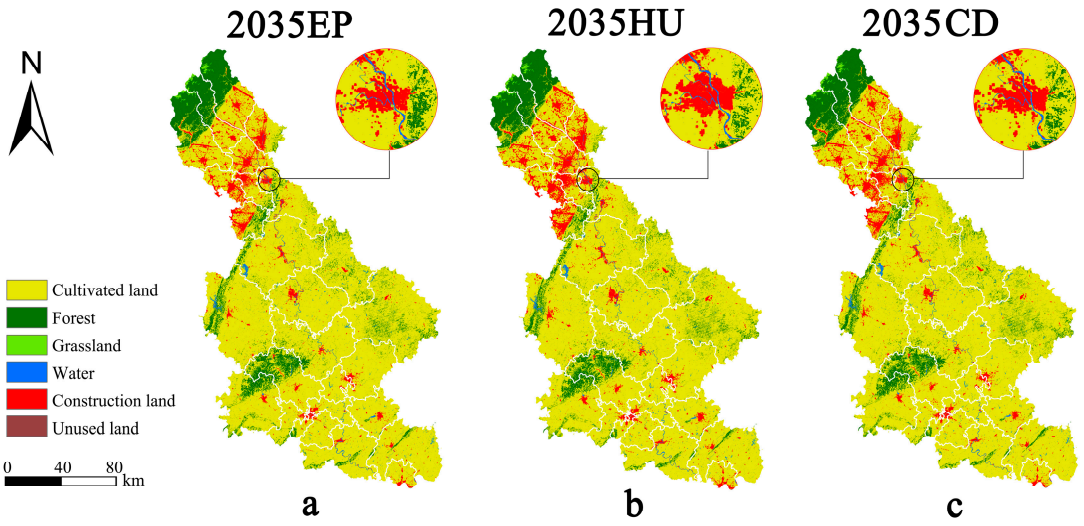


Figure 4. Simulations of land-use change under different scenarios in the Tuojiang River Basin in 2035. Note: (**a**) EP: ecological priority scenario; (**b**) HU: high urbanization scenario; (**c**) CD: coordinated development scenario.

Land in the three scenarios exhibited a spatial distribution pattern characterized by differentiation (Figure 4). Regarding the type of land conversion, the magnitude of transformation from cultivated land to construction land varied as follows: HU > CD > EP. For other land conversion types, the differences in conversion quantities across different scenarios were relatively small. The largest conversion occurred from cultivated land to forestland and from construction land to cultivated land in the EP scenario, whereas the conversions from cultivated land to water bodies and from forestland to cultivated land were the most significant in the HU scenario.

3.2. Carbon Storage Dynamics during 2000–2035

3.2.1. Carbon Storage Dynamics during 2000 to 2020

The simulated carbon storage in the TRB was estimated at 664.70 Tg for 2000, 662.36 Tg for 2010, and 674.39 Tg for 2020. The carbon storage trend displayed a decline at first, followed by a subsequent increase. The spatial distribution of carbon storage demonstrated notable heterogeneity across the TRB (Figure 5). Areas exhibiting high carbon storage values were predominantly concentrated in the Pengzhou mountainous region upstream of the TRB and the Qionglong mountainous region downstream of the TRB. These areas are primarily covered by forests and exhibit strong carbon sequestration capacity.

The regions that experienced notable increases in carbon storage from 2000 to 2020 were predominantly centered in the Qionglong mountainous region downstream of the TRB (Figure 5b). Regions with decreased carbon storage are primarily located in the Chengdu Plain area in the upstream reaches of the TRB. From 2000 to 2010, areas exhibiting increased carbon storage were primarily situated in the Longmen mountainous region in the middle reaches of the TRB and the Qionglong mountainous region in the lower reaches of the TRB. The decline in carbon storage was predominantly observed in the upper reaches of the TRB, specifically in the Pengzhou mountainous region and the Chengdu Plain (Figure 5c). After 2010, there was a significant expansion in areas undergoing carbon storage changes. The regions with increased carbon storage were mainly concentrated in the Pengzhou mountainous region in the upper reaches of the TRB, the Longmen mountainous region in the middle reaches, and the Qionglong mountainous region in the lower reaches. Decreases in carbon storage were scattered, predominantly in the Chengdu Plain area of the upper reaches, as well as in the hilly regions of the middle and lower reaches of the TRB (Figure 5d).

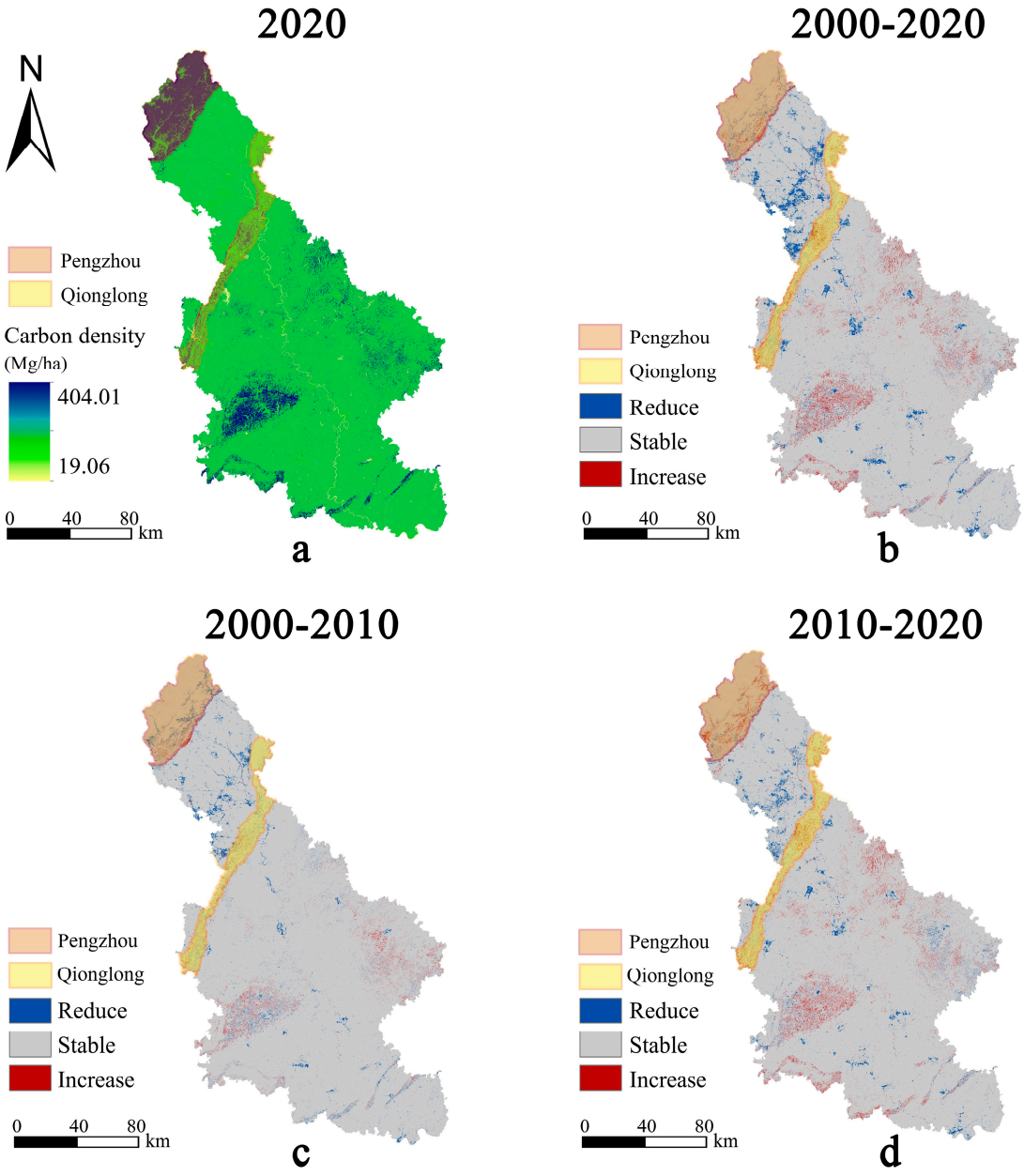


Figure 5. (**a**) Spatial heterogeneity of carbon storage in the Tuojiang River Basin in 2020; (**b**–**d**) areas depicting changes in carbon storage.

3.2.2. Dynamics of Carbon Storage across Various Scenarios

In 2035, the total carbon storage of the TRB under EP, HU, and CD will be 676.23 Tg, 674.06 Tg, and 675.18 Tg, respectively (Figure 6). Under the EP scenario, the total carbon storage and average carbon density of the TRB in 2035 increased by 1.84 Tg and 0.62 Mg·ha^{-1} compared to 2020, respectively (Table 4). Under the CD scenario, the total carbon storage and average carbon density of the TRB in 2035 increased by 0.79 Tg and 0.27 Mg·ha^{-1} compared to 2020, respectively. In the CD scenario, the carbon storage in cultivated land decreased by 16.85 Tg, while the carbon storage in forest and construction land increased by 3.10 Tg and 14.87 Tg, respectively (Table S5). When under the HU scenario, the total carbon storage and average carbon density in the study area were 0.33 Tg and 0.11 Mg·ha^{-1} lower than the values in 2020, respectively. In the HU scenario, the carbon storage in cultivated land decreased by 20.93 Tg, while the carbon storage in forest and construction land increased by 1.33 Tg and 19.59 Tg, respectively. Overall, under the EP scenario, carbon storage showed the largest growth magnitude and highest carbon density,

mainly due to the transition of forestland with higher carbon density under this scenario. In the EP scenario, the carbon storage in cultivated land decreased by 12.97 Tg, while the carbon storage in forest and construction land increased by 4.84 Tg and 10.31 Tg, respectively. These decreases were specific to the HU scenario, indicating that rapid urbanization causes a decline in carbon storage.

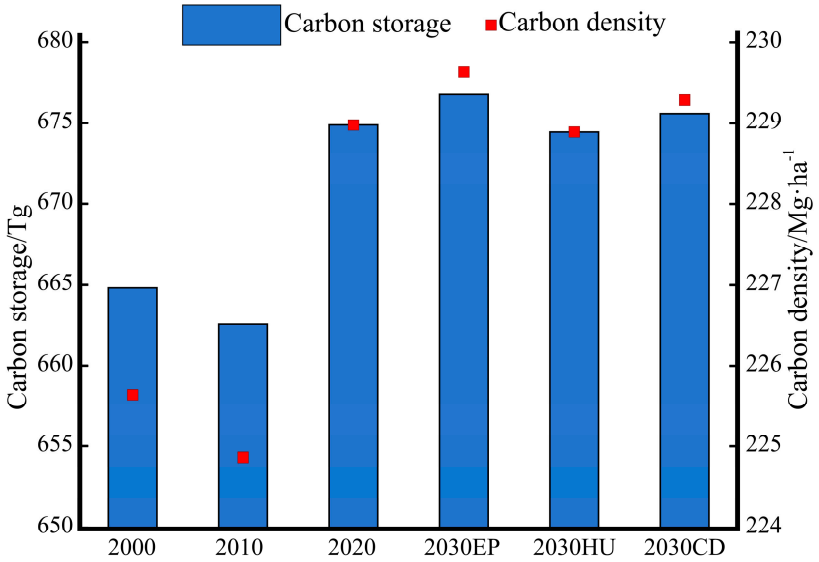


Figure 6. Changes in total carbon storage and average density in the Tuojiang River Basin. Note: EP: ecological priority scenario; HU: high urbanization scenario; CD: coordinated development scenario.

Table 4. Carbon storage (Tg) corresponding to different land-use types in the Tuojiang River Basin from 2000 to 2035.

Year	**Land Use Types**					
	2000	2010	2020	2035EP	2035HU	2035CD
Cultivated land	546.36	539.73	518.19	505.22	497.27	501.34
Forest	108.09	106.28	130.55	135.39	131.87	133.64
Grassland	2.28	2.42	2.42	2.19	2.19	2.19
Water	0.59	0.72	0.65	0.65	0.66	0.66
Construction land	7.34	13.14	22.42	32.73	42.01	37.30
Unused land	0.04	0.07	0.16	0.05	0.06	0.05

In the three 2035 scenarios, the decline in carbon storage is concentrated in the Chengdu Plain region of the upper reaches of the TRB (Figure 7). These changes arise from frequent anthropogenic activities and significant alterations in land-use patterns. In particular, the transition of forestland to cultivated land results in a reduction in carbon storage [49]. Under the HU scenario, the notable decline in carbon storage was attributed to the extensive enlargement of construction land within the core economic activity zones, where the shift from high-carbon-density cultivated land to low-carbon-density construction land will be more evident. The areas with increased carbon storage were mainly distributed in the Pengzhou mountainous area of the upper reaches, Longmen mountainous area of the middle reaches, and Qionglong mountainous and hilly areas of the lower reaches of the TRB. The carbon storage increase was the most prominent under the EP scenario. Under the EP scenario, forest areas with higher carbon density and cultivated land will both expand, while the expansion of construction land will slow down in the Chengdu Plain region of the upper reaches of the TRB.

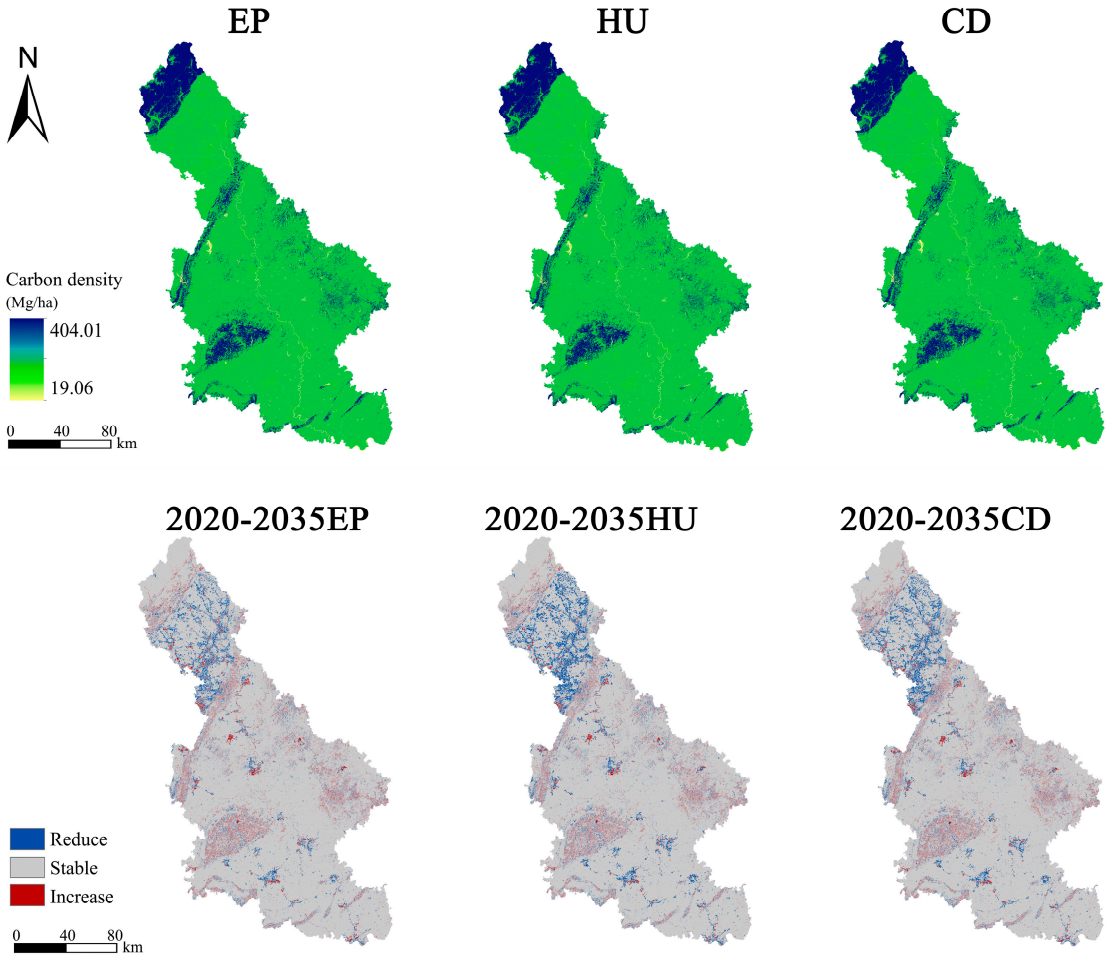


Figure 7. Changes in the spatial distribution of carbon storage in the Tuojiang River Basin under three scenarios.

3.3. Spatial Distribution Characteristics of Carbon Storage

The spatial autocorrelation analysis method was applied to assess the average carbon density at the town level under three scenarios, with the aim of uncovering the spatial agglomeration features of carbon storage under prospective scenarios within the TRB. In the EP and CD scenarios, the high–high clusters of carbon storage in the TRB were primarily concentrated in mountainous areas of the upper and lower streams of the TRB, with some sporadically scattered in the middle reaches (Figure 8). The Pengzhou mountainous area in the upper reaches and the Qionglong mountainous region in the lower reaches of the TRB, characterized by the largest forest coverage area, represent the most substantial high–high agglomeration areas. The high aggregation was not prominent within the whole basin. In the HU scenario, the high–low cluster area of carbon storage was located in the Pengzhou mountainous area and sporadically scattered in the middle and lower hill regions.

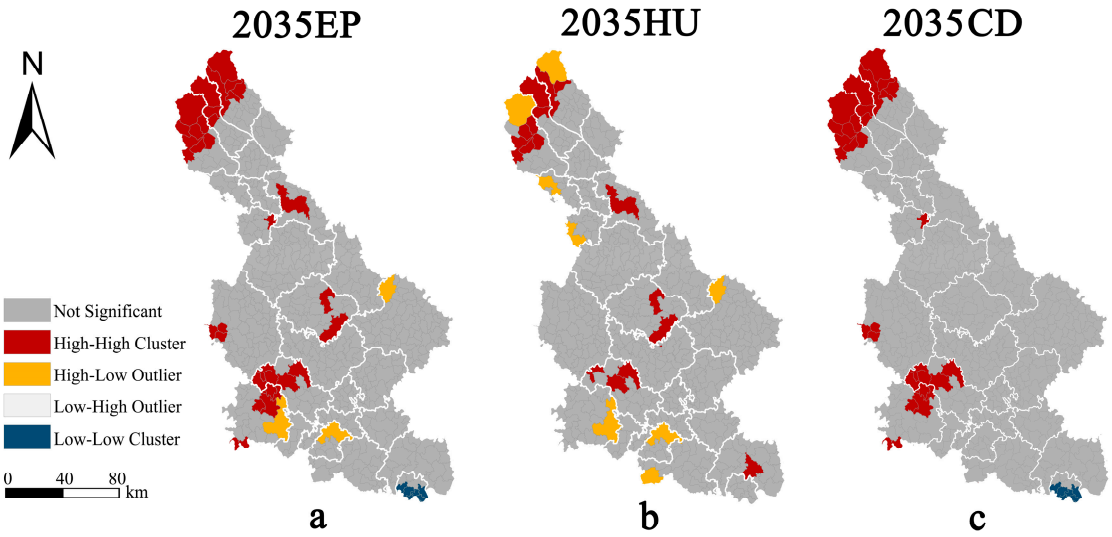


Figure 8. LISA clustering of carbon storage under (**a**) EP, (**b**) HU, and (**c**) CD scenarios of 2035 in the Tuojiang River Basin.

4. Discussion

4.1. Influence of LUCC on Carbon Storage in the TRB

Terrestrial carbon sequestration is influenced by land-use changes, which can function directly or indirectly as carbon sources or sinks [50,51]. Analyzing the influence of LUCC on carbon storage provides a crucial framework for guiding future land utilization strategies toward the attainment of carbon neutrality goals. Over the past two decades, accelerated socioeconomic development in the primary urban areas of the TRB, combined with frequent human activities [32,52], has triggered rapid urbanization. The rapid development has greatly escalated the need for urban construction, leading to the transformation of a large portion of cultivated land into built-up areas. This transition from cultivated land with higher carbon density to construction land with lower carbon density has led to a decrease in regional carbon density and the overall carbon storage capacity (Figure 5). These findings are in line with those of Xiang, et al. [53] and Seto, et al. [54], who identified a decreasing trend in carbon storage associated with the conversion of cultivated land to construction land in heavily populated areas over the past few decades. The increase in carbon storage in the TRB from 2010 to 2020 was predominantly ascribed to the deliberate execution of ecological protection initiatives [55]. This offsets the decline in carbon storage caused by the conversion of cultivated land to construction land, leading to an increase in carbon storage and density in the watershed between 2010 and 2020 (Figure 6). Overall, the transition of the LUCC within the TRB from 2000 to 2020 significantly influenced carbon storage, and the optimization of future LUCC assumes pivotal significance.

4.2. Suggestions for Future Land-Use Optimization in the TRB

The forthcoming trends and spatial patterns of carbon storage in the TRB varied substantially among the three distinct scenarios, contingent on the specifications and constraints inherent in each development scenario. Based on the results of the LUCC simulation in the TRB for 2035, an estimation conducted using the InVEST model highlighted an increase in carbon storage across the EP and CD scenarios. Notably, the EP scenario exhibited the highest recorded carbon storage, primarily attributed to the effective implementation of ecological protection policies. This transition substantially enhanced carbon storage in the mountainous forest zone of the TRB. However, the carbon storage exhibited a declining trend in the HU scenario. This was due to a significant decrease in cultivated land and a rise in construction land in the upper basin, which drove the shift from high-carbon-density cultivated land to low-carbon-density construction land, ultimately resulting in reduced carbon storage within the TRB. Similar results have been observed in other projections

of carbon storage under scenarios of rapid urbanization [56,57]. Unlike the EP and HU scenarios, the CD scenario sets itself apart by encompassing vast areas of cultivated land and construction. Remarkably, it underwent a moderate expansion in built-up land while simultaneously demonstrating a rise in carbon stocks. The CD scenario achieved a delicate balance between urban development and ecological conservation, offering a foundation for attaining regional carbon neutrality through strategic planning.

In the upper reaches of the basin, the Chengdu Plain region exhibits significant land intensification and fragmentation, primarily dominated by cultivated and construction land, thus limiting its capacity for high-density carbon storage. Previous studies have demonstrated that efficient farmland management (e.g., straw returning) can significantly enhance carbon sequestration within agricultural ecosystems [58]. The policy of returning straw to fields is imperative to promote low-carbon agriculture to convert the scale advantage of arable land into a carbon sink advantage. The assessment of carbon storage stability under the three scenarios suggests that the most significant changes will likely be concentrated in the rapidly expanding urban zones of the upper TRB. Controlling the expansion of construction land while simultaneously increasing urban green coverage should be considered to enhance regional carbon sink capacity. Land use for construction should transition from expansion to optimizing existing resources, continuously improving efficiency and intensification, thereby conserving more arable and ecological land. In contrast, areas with the highest concentration and lowest susceptibility to change were the protected zones within the mountainous regions situated in the upper reaches of the TRB, where mountainous terrain and elevated topography impede the expansion of construction land. Consequently, areas with high-value carbon storage are extensively concentrated in significantly forested areas, exhibiting robust carbon sequestration capabilities and representing the largest carbon sink within ecosystems [59,60]. Therefore, it is recommended that rigorous national Ecological Conservation Redline policy and strategic planning be implemented to enlarge the ecological land in these areas. Targeted efforts should focus on the ecological protection and restoration of the Pengzhou and Qionglong mountain ranges, implementing measures for forest tending and the restoration of degraded forests to elevate the carbon sink capacity of these mountainous ecological barriers.

4.3. Uncertainty and Future Perspectives

Initially, the InVEST model offered advantages, including flexible parameters, straightforward operation, dynamic capabilities, and spatialization [61]. The InVEST model also has certain limitations, such as not accounting for interannual variations in carbon density and the lack of verification of carbon density using field sampling data. However, conducting field sampling and surveys is costly and challenging, particularly when dealing with extensive study areas [62]. Our study attempted to calibrate the carbon density by incorporating field sampling data from previous research in adjacent regions. Calibration of the coefficients was also combined with meteorological data to minimize errors in the carbon storage assessments. Notably, marginal annual variations observed in regional carbon density data had negligible effects on the estimation of carbon storage in extensive terrestrial ecosystems, as demonstrated in a previous study [22]. Future research could boost model precision by utilizing multiyear dynamic carbon density data gathered from continuous monitoring or field investigations [63].

Climate change may influence the turnover of soil organic carbon, subsequently affecting soil carbon storage [64,65]. However, this study did not account for this factor due to the limited impact of climate change on relatively small regions over short time scales. In future studies, the potential effects of climate change on soil carbon storage should be considered, particularly over larger spatial scales.

Ecosystem services include provisioning, regulation, and cultural services [66]. In future research, particularly focusing on watershed areas, it will be crucial to explore the significant ecosystem service characteristics related to comprehensive provisioning services (such as water and food production) and soil retention. This coupled model framework is

adaptable to a broad range of geographic contexts, with particular suitability for longer time scales or larger spatial scales due to its flexible design and adjustable parameters.

5. Conclusions

In this research, we simulated LUCCs in the TRB under various scenarios using the SD-PLUS-InVEST coupled model to estimate its effect on changes in carbon storage. From 2000 to 2020, the LUCC in the TRB experienced notable transformations, with cultivated land primarily transitioning into forest and construction land. The carbon storage exhibited a trend of initially decreasing and subsequently increasing during this period. Regions with reduced carbon storage are particularly conspicuous in the Chengdu Plain region within the upper reaches of the TRB.

By 2035, total carbon storage in the TRB will show an increasing trend in the EP and SD scenarios. However, carbon storage decreases in the HU scenario, indicating that rapid urbanization will cause a decline in carbon storage. The regions with the highest carbon storage were mainly located in the mountainous areas of the basin, which are predominantly characterized by forested landscapes. Conversely, the lowest carbon storage areas were primarily found in the Chengdu Plain, located in the upper part of the basin. The CD scenario can achieve balance by meeting the demand for economic development while simultaneously sustaining an increase in carbon storage. Our results indicate that future development strategies should prioritize ecological protection and coordinated development. These findings have practical implications and are relevant to policymaking, offering valuable insights into LULC changes and the achievement of carbon neutrality in the TRB and comparable regions.

Supplementary Materials: The following supporting information can be downloaded at: https://www.mdpi.com/article/10.3390/land13091518/s1, Figure S1: Causal Loop Diagram of Main Elements of Man-land System in Tuojiang River Basin; Figure S2: The SD model's causal feedback chart of land use demand change in the Tuojiang River Basin; Table S1: SD model variables of Tuojiang River Basin; Table S2: Ecological priority scenario parameters; Table S3: Highly urbanization scenario parameters; Table S4: Coordinated development scenario parameters. Table S5. Change of carbon storage across different land use types from 2020 to 2035 (Tg).

Author Contributions: Q.W.: Conceptualization, methodology, data curation, drawing, writing—review and editing; W.Z.: data curation, drawing, software, validation; J.X.: data curation, methodology; D.O.: drawing, software; Z.T.: drawing, reviewing and editing; X.G.: conceptualization, reviewing and editing, funding acquisition, project administration. All authors have read and agreed to the published version of the manuscript.

Funding: This research was funded by the Ministry of Science and Technology of China, National Key Research and Development Plan (grant number 2022YFD1901400).

Data Availability Statement: The data that support the findings of this study are available on request from the corresponding author.

Acknowledgments: The authors thank the anonymous reviewers for the helpful comments that improved this manuscript.

Conflicts of Interest: The authors declare no conflicts of interest.

References

1. Hoegh-Guldberg, O.; Jacob, D.; Taylor, M.; Guillén Bolaños, T.; Bindi, M.; Brown, S.; Camilloni, I.A.; Diedhiou, A.; Djalante, R.; Ebi, K.; et al. The human imperative of stabilizing global climate change at 1.5 °C. *Science* **2019**, *365*, eaaw6974. [CrossRef]
2. Liu, Z.; Deng, Z.; He, G.; Wang, H.; Zhang, X.; Lin, J.; Qi, Y.; Liang, X. Challenges and opportunities for carbon neutrality in China. *Nat. Rev. Earth Environ.* **2022**, *3*, 141–155. [CrossRef]
3. Lal, R.; Smith, P.; Jungkunst, H.F.; Mitsch, W.J.; Lehmann, J.; Nair, P.R.; McBratney, A.B.; de Moraes Sá, J.C.; Schneider, J.; Zinn, Y.L.; et al. The carbon sequestration potential of terrestrial ecosystems. *J. Soil Water Conserv.* **2018**, *73*, 145A–152A. [CrossRef]
4. Wang, F.; Harindintwali, J.D.; Yuan, Z.; Wang, M.; Wang, F.; Li, S.; Yin, Z.; Huang, L.; Fu, Y.; Li, L. Technologies and perspectives for achieving carbon neutrality. *Innovation* **2021**, *2*, 100180. [CrossRef]

5. He, C.; Zhang, D.; Huang, Q.; Zhao, Y. Assessing the potential impacts of urban expansion on regional carbon storage by linking the LUSD-urban and InVEST models. *Environ. Model. Softw.* **2016**, *75*, 44–58. [CrossRef]
6. Lal, R.; Negassa, W.; Lorenz, K. Carbon sequestration in soil. *Curr. Opin. Environ. Sustain.* **2015**, *15*, 79–86. [CrossRef]
7. Deng, L.; Zhu, G.-Y.; Tang, Z.-S.; Shangguan, Z.-P. Global patterns of the effects of land-use changes on soil carbon stocks. *Glob. Ecol. Conserv.* **2016**, *5*, 127–138. [CrossRef]
8. Ma, K.; Zhang, Y.; Tang, S.; Liu, J. Spatial distribution of soil organic carbon in the Zoige alpine wetland, northeastern Qinghai–Tibet Plateau. *Catena* **2016**, *144*, 102–108. [CrossRef]
9. Laganiere, J.; Angers, D.A.; Pare, D. Carbon accumulation in agricultural soils after afforestation: A meta-analysis. *Glob. Change Biol.* **2010**, *16*, 439–453. [CrossRef]
10. Fallahzade, J.; Hajabbasi, M. The effects of irrigation and cultivation on the quality of desert soil in central Iran. *Land Degrad. Dev.* **2012**, *23*, 53–61. [CrossRef]
11. Ren, Y.; Lü, Y.; Comber, A.; Fu, B.; Harris, P.; Wu, L. Spatially explicit simulation of land use/land cover changes: Current coverage and future prospects. *Earth-Sci. Rev.* **2019**, *190*, 398–415. [CrossRef]
12. Yin, Y.; Yang, R.; Song, Z.; Lu, Y.; Zhang, Y.; Zhang, L.; Sun, M.; Li, X. Simulation of wetland carbon storage in coastal cities under the coupled framework of socio-economic and ecological sustainability: A case study of Dongying city. *Sustain. Cities Soc.* **2024**, *108*, 105481. [CrossRef]
13. Gomes, E.; Inácio, M.; Bogdzevič, K.; Kalinauskas, M.; Karnauskaitė, D.; Pereira, P. Future land-use changes and its impacts on terrestrial ecosystem services: A review. *Sci. Total Environ.* **2021**, *781*, 146716. [CrossRef]
14. Liang, X.; Liu, X.; Li, X.; Chen, Y.; Tian, H.; Yao, Y. Delineating multi-scenario urban growth boundaries with a CA-based FLUS model and morphological method. *Landsc. Urban Plan.* **2018**, *177*, 47–63. [CrossRef]
15. Chanapathi, T.; Thatikonda, S. Investigating the impact of climate and land-use land cover changes on hydrological predictions over the Krishna river basin under present and future scenarios. *Sci. Total Environ.* **2020**, *721*, 137736. [CrossRef]
16. De Rosa, M.; Knudsen, M.T.; Hermansen, J.E. A comparison of Land Use Change models: Challenges and future developments. *J. Clean. Prod.* **2016**, *113*, 183–193. [CrossRef]
17. Schoenenberger, L.; Schmid, A.; Tanase, R.; Beck, M.; Schwaninger, M. Structural analysis of system dynamics models. *Simul. Model. Pract. Theory* **2021**, *110*, 102333. [CrossRef]
18. Zomorodian, M.; Lai, S.H.; Homayounfar, M.; Ibrahim, S.; Fatemi, S.E.; El-Shafie, A. The state-of-the-art system dynamics application in integrated water resources modeling. *J. Environ. Manag.* **2018**, *227*, 294–304. [CrossRef]
19. Liang, X.; Guan, Q.; Clarke, K.C.; Liu, S.; Wang, B.; Yao, Y. Understanding the drivers of sustainable land expansion using a patch-generating land use simulation (PLUS) model: A case study in Wuhan, China. *Comput. Environ. Urban* **2021**, *85*, 101569. [CrossRef]
20. Chen, Q.; Ning, Y. Projecting LUCC dynamics and ecosystem services in an emerging urban agglomeration under SSP-RCP scenarios and their management implications. *Sci. Total Environ.* **2024**, *949*, 175100. [CrossRef]
21. Zhang, Z.; Li, X.; Liu, X.; Zhao, K. Dynamic simulation and projection of land use change using system dynamics model in the Chinese Tianshan mountainous region, central Asia. *Ecol. Model.* **2024**, *487*, 110564. [CrossRef]
22. Tang, X.; Zhao, X.; Bai, Y.; Tang, Z.; Wang, W.; Zhao, Y.; Wan, H.; Xie, Z.; Shi, X.; Wu, B. Carbon pools in China's terrestrial ecosystems: New estimates based on an intensive field survey. *Proc. Natl. Acad. Sci. USA* **2018**, *115*, 4021–4026. [CrossRef] [PubMed]
23. Campbell, A.D.; Fatoyinbo, T.; Charles, S.P.; Bourgeau-Chavez, L.L.; Goes, J.; Gomes, H.; Halabisky, M.; Holmquist, J.; Lohrenz, S.; Mitchell, C. A review of carbon monitoring in wet carbon systems using remote sensing. *Environ. Res. Lett.* **2022**, *17*, 025009. [CrossRef]
24. Stockmann, U.; Adams, M.A.; Crawford, J.W.; Field, D.J.; Henakaarchchi, N.; Jenkins, M.; Minasny, B.; McBratney, A.B.; De Courcelles, V.d.R.; Singh, K. The knowns, known unknowns and unknowns of sequestration of soil organic carbon. *Agric. Ecosyst. Environ.* **2013**, *164*, 80–99. [CrossRef]
25. Evans, T.P.; Robinson, D.T.; Schmitt-Harsh, M. The carbon cycle: Advances in Integrated Science. In *Limitations, Challenges, and Solutions to Integrating Carbon Dynamics with Land-Use Models*; Brown, D.G., Robinson, D.T., French, N.H.F., Reed, B.C., Eds.; Cambridge University Press: Cambridge, UK, 2013; pp. 178–208.
26. He, Y.; Ma, J.; Zhang, C.; Yang, H. Spatio-Temporal Evolution and Prediction of Carbon Storage in Guilin Based on FLUS and InVEST Models. *Remote Sens.* **2023**, *15*, 1445. [CrossRef]
27. Ismaili Alaoui, H.; Chemchaoui, A.; El Asri, B.; Ghazi, S.; Brhadda, N.; Ziri, R. Modeling predictive changes of carbon storage using invest model in the Beht watershed (Morocco). *J. Adv. Model. Earth Syst.* **2023**, *9*, 4313–4322. [CrossRef]
28. Shen, J.; Li, S.; Liu, L.; Liang, Z.; Wang, Y.; Wang, H.; Wu, S. Uncovering the relationships between ecosystem services and social-ecological drivers at different spatial scales in the Beijing-Tianjin-Hebei region. *J. Clean. Prod.* **2021**, *290*, 125193. [CrossRef]
29. Lumeng, L.; Jianguo, W. Scenario analysis in urban ecosystem services research: Progress, prospects, and implications for urban planning and management. *Landsc. Urban Plan.* **2022**, *224*, 104433. [CrossRef]
30. Zhong, X.; Zhang, S.; Wu, R.; Jing, Y.; Men, L.; Zhou, T. Analysis of dynamic changes and driving forces of soil erosion in tuojiang river basin. *Res. Soil Water Conserv.* **2022**, *29*, 43–56.

31. Wang, Q.; Le Noë, J.; Li, Q.; Lan, T.; Gao, X.; Deng, O.; Li, Y. Incorporating agricultural practices in digital mapping improves prediction of cropland soil organic carbon content: The case of the Tuojiang River Basin. *J. Environ. Manag.* **2023**, *330*, 117203. [CrossRef]
32. Wang, Q.; Gao, X.; Li, Q.; Lan, T.; Huang, R.; Deng, O. Spatially explicit reconstruction of the population distribution in the Tuojiang River Basin during 1911–2010 using random forest regression. *Reg. Environ. Chang.* **2022**, *22*, 13. [CrossRef]
33. Allan, A.; Soltani, A.; Abdi, M.H.; Zarei, M. Driving forces behind land use and land cover change: A systematic and bibliometric review. *Land* **2022**, *11*, 1222. [CrossRef]
34. Yang, J.; Huang, X. The 30 m annual land cover dataset and its dynamics in China from 1990 to 2019. *Earth Syst. Sci. Data* **2021**, *13*, 3907–3925. [CrossRef]
35. Yang, Y.; Bao, W.; Liu, Y. Scenario simulation of land system change in the Beijing-Tianjin-Hebei region. *Land Use Policy* **2020**, *96*, 104677. [CrossRef]
36. Liang, X.; Guan, Q.; Clarke, K.C.; Chen, G.; Guo, S.; Yao, Y. Mixed-cell cellular automata: A new approach for simulating the spatio-temporal dynamics of mixed land use structures. *Landsc. Urban Plan.* **2021**, *205*, 103960. [CrossRef]
37. Yao, Y.; Liu, X.; Li, X.; Liu, P.; Hong, Y.; Zhang, Y.; Mai, K. Simulating urban land-use changes at a large scale by integrating dynamic land parcel subdivision and vector-based cellular automata. *Int. J. Geogr. Inf. Sci.* **2017**, *31*, 2452–2479. [CrossRef]
38. He, J.; Li, X.; Yao, Y.; Hong, Y.; Jinbao, Z. Mining transition rules of cellular automata for simulating urban expansion by using the deep learning techniques. *Int. J. Geogr. Inf. Sci.* **2018**, *32*, 2076–2097. [CrossRef]
39. Wang, C.; Li, T.; Guo, X.; Xia, L.; Lu, C.; Wang, C. Plus-InVEST Study of the Chengdu-Chongqing urban agglomeration's land-use change and carbon storage. *Land* **2022**, *11*, 1617. [CrossRef]
40. Hu, S.; Zhang, X.; Guan, D. Analysis on carbon storage change of construction land expansion in chongqing based on InVEST model. *Res. Soil Water Conserv.* **2018**, *25*, 323–331. [CrossRef]
41. Xiang, M.; Wang, C.; Tan, Y.; Yang, J.; Duan, L.; Fang, Y.; Li, W.; Shu, Y.; Liu, M. Spatio-temporal evolution and driving factors of carbon storage in the Western Sichuan Plateau. *Sci. Rep.* **2022**, *12*, 8114. [CrossRef]
42. Huang, C.-D.; Zhang, J.; Yang, W.-Q.; Tang, X. Spatiotemporal variation of carbon storage in forest vegetation in Sichuan Province. *Chin. J. Appl. Ecol.* **2007**, *18*, 2687–2692.
43. Wang, X.; Zhou, M.; Li, T.; Ke, Y.; Zhu, B. Land use change effects on ecosystem carbon budget in the Sichuan Basin of Southwest China: Conversion of cropland to forest ecosystem. *Sci. Total Environ.* **2017**, *609*, 556–562. [CrossRef] [PubMed]
44. Wiesmeier, M.; Urbanski, L.; Hobley, E.; Lang, B.; von Lützow, M.; Marin-Spiotta, E.; van Wesemael, B.; Rabot, E.; Ließ, M.; Garcia-Franco, N. Soil organic carbon storage as a key function of soils-A review of drivers and indicators at various scales. *Geoderma* **2019**, *333*, 149–162. [CrossRef]
45. Xu, C.; Zhang, Q.; Yu, Q.; Wang, J.; Wang, F.; Qiu, S.; Ai, M.; Zhao, J. Effects of land use/cover change on carbon storage between 2000 and 2040 in the Yellow River Basin, China. *Ecol. Indic.* **2023**, *151*, 110345. [CrossRef]
46. Alam, S.A.; Starr, M.; Clark, B.J. Tree biomass and soil organic carbon densities across the Sudanese woodland savannah: A regional carbon sequestration study. *J. Arid. Environ.* **2013**, *89*, 67–76. [CrossRef]
47. Cai, G.; Xiong, J.; Wen, L.; Weng, A.; Lin, Y.; Li, B. Predicting the ecosystem service values and constructing ecological security patterns in future changing land use patterns. *Ecol. Indic.* **2023**, *154*, 110787. [CrossRef]
48. Liu, X.; Liang, X.; Li, X.; Xu, X.; Ou, J.; Chen, Y.; Li, S.; Wang, S.; Pei, F. A future land use simulation model (FLUS) for simulating multiple land use scenarios by coupling human and natural effects. *Landsc. Urban Plan.* **2017**, *168*, 94–116. [CrossRef]
49. Ge, Q.; Dai, J.; He, F.; Pan, Y.; Wang, M. Land use changes and their relations with carbon cycles over the past 300 a in China. *Sci. China Earth Sci.* **2008**, *51*, 871–884. [CrossRef]
50. Thangavel, R.; Bolan, N.S.; Kirkham, M.B.; Wijesekara, H.; Manjaiah, K.; Rao, C.S.; Sasidharan, S.; Rinklebe, J.; Ok, Y.; Choudhury, B.U. Soil organic carbon dynamics: Impact of land use changes and management practices: A review. *Adv. Agron.* **2019**, *156*, 1–107. [CrossRef]
51. Keenan, T.; Williams, C. The terrestrial carbon sink. *Annu. Rev. Environ. Resour.* **2018**, *43*, 219–243. [CrossRef]
52. Wang, Q.; Xiong, M.; Li, Q.; Li, H.; Lan, T.; Deng, O.; Huang, R.; Zeng, M.; Gao, X. Spatially explicit reconstruction of cropland using the random forest: A case study of the Tuojiang River Basin, China from 1911 to 2010. *Land* **2021**, *10*, 1338. [CrossRef]
53. Xiang, S.; Wang, Y.; Deng, H.; Yang, C.; Wang, Z.; Gao, M. Response and multi-scenario prediction of carbon storage to land use/cover change in the main urban area of Chongqing, China. *Ecol. Indic.* **2022**, *142*, 109205. [CrossRef]
54. Seto, K.C.; Güneralp, B.; Hutyra, L.R. Global forecasts of urban expansion to 2030 and direct impacts on biodiversity and carbon pools. *Proc. Natl. Acad. Sci. USA* **2012**, *109*, 16083–16088. [CrossRef] [PubMed]
55. Chen, X.; Yu, L.; Du, Z.; Xu, Y.; Zhao, J.; Zhao, H.; Zhang, G.; Peng, D.; Gong, P. Distribution of ecological restoration projects associated with land use and land cover change in China and their ecological impacts. *Sci. Total Environ.* **2022**, *825*, 153938. [CrossRef] [PubMed]
56. Wang, Y.; Liang, D.; Wang, J.; Zhang, Y.; Chen, F.; Ma, X.J. An analysis of regional carbon stock response under land use structure change and multi-scenario prediction, a case study of Hefei, China. *Ecol. Indic.* **2023**, *151*, 110293. [CrossRef]
57. Li, Z.-T.; Li, M.; Xia, B.C. Spatio-temporal dynamics of ecological security pattern of the Pearl River Delta urban agglomeration based on LUCC simulation. *Ecol. Indic.* **2020**, *114*, 106319. [CrossRef]

58. Wang, Q.; Barré, P.; Li, Q.; Lan, T.; Zhou, M.; Gao, X.; Le Noë, J. Multi-decadal and regional validation of the AMG model at county and grid scales unravels the role of crop residue inputs in increasing soil organic carbon stocks in the Tuojiang River Basin, China. *Agric. Ecosyst. Environ.* **2024**, *371*, 109092. [CrossRef]
59. Pan, Y.; Birdsey, R.A.; Fang, J.; Houghton, R.; Kauppi, P.E.; Kurz, W.A.; Phillips, O.L.; Shvidenko, A.; Lewis, S.L.; Canadell, J.G. Science A large and persistent carbon sink in the world's forests. *Proc. Natl. Acad. Sci. USA* **2011**, *333*, 988–993. [CrossRef]
60. Pugh, T.A.; Lindeskog, M.; Smith, B.; Poulter, B.; Arneth, A.; Haverd, V.; Calle, L. Role of forest regrowth in global carbon sink dynamics. *Proc. Natl. Acad. Sci. USA* **2019**, *116*, 4382–4387. [CrossRef]
61. Li, P.; Chen, J.; Li, Y.; Wu, W. Using the InVEST-PLUS Model to Predict and Analyze the Pattern of Ecosystem Carbon storage in Liaoning Province, China. *Remote Sens.* **2023**, *15*, 4050. [CrossRef]
62. Hu, X.; Hou, Y.; Li, D.; Hua, T.; Marchi, M.; Urrego, J.P.F.; Huang, B.; Zhao, W.; Cherubini, F. Changes in multiple ecosystem services and their influencing factors in Nordic countries. *Ecol. Indic.* **2023**, *146*, 109847. [CrossRef]
63. Elliot, T.; Bertrand, A.; Almenar, J.B.; Petucco, C.; Proença, V.; Rugani, B. Spatial optimisation of urban ecosystem services through integrated participatory and multi-objective integer linear programming. *Ecol. Indic.* **2019**, *409*, 108774. [CrossRef]
64. Rodrigues, C.I.D.; Brito, L.M.; Nunes, L.J. Soil carbon sequestration in the context of climate change mitigation: A review. *Soil Syst.* **2023**, *7*, 64. [CrossRef]
65. Luo, Z.; Feng, W.; Luo, Y.; Baldock, J.; Wang, E. Soil organic carbon dynamics jointly controlled by climate, carbon inputs, soil properties and soil carbon fractions. *Glob. Chang. Biol.* **2017**, *23*, 4430–4439. [CrossRef]
66. Rimal, B.; Sharma, R.; Kunwar, R.; Keshtkar, H.; Stork, N.E.; Rijal, S.; Rahman, S.A.; Baral, H. Effects of land use and land cover change on ecosystem services in the Koshi River Basin, Eastern Nepal. *Ecosyst. Serv.* **2019**, *38*, 100963. [CrossRef]

Disclaimer/Publisher's Note: The statements, opinions and data contained in all publications are solely those of the individual author(s) and contributor(s) and not of MDPI and/or the editor(s). MDPI and/or the editor(s) disclaim responsibility for any injury to people or property resulting from any ideas, methods, instructions or products referred to in the content.